Rheooptical Determination of Aspect Ratio and Polydispersity of Nonspherical Particles

J. Vermant and H. Yang
Dept. of Chemical Engineering, K.U. Leuven, 3001 Leuven, Belgium

G. G. Fuller
Dept. of Chemical Engineering, Stanford University, Stanford, CA 94305

A rheooptical method proposed rapidly determines the aspect ratio and polydispersity of small axisymmetric, nonspherical particles. The time evolution of the average orientation angle of optically isotropic, nonabsorbing particles upon inception of a shear flow was monitored by a polarization modulation method by using dilute suspensions of the particles. Since the orientation angle is a geometric property of the particles, no arbitrary assumptions on the scattering mechanism had to be made to analyze the data. The period of the damped oscillatory response of the orientation angle is related to the average aspect ratio. In the limit of strong flows the damping only depends on dispersion in particle shape. An analytical expression to relate the polydispersity of the equivalent hydrodynamic aspect ratio to the damping function is presented, as well as the applicability of the technique by studying the hydrodynamic aspect ratio and associated polydispersity in a sample containing ellipsoidal hematite particles.

Introduction

It is often important to know the size and shape of colloidal particles, as they have a strong effect on the rheological, optical, and/or mechanical properties of suspensions (Hiemenz and Rajagopalan, 1997). However, rapidly determining the geometrical aspects of small nonspherical particles is not straightforward. Preparation of samples for electron microscopy is often laborious and expensive and the analysis of the images is not trivial. Special problems occur when the particles aggregate during evaporation of the dispersion medium. In addition, it is sometimes desirable to determine the geometry of particles in a fluid, with the possible formation of doublets or aggregates. Light-scattering methods, as used in many commercial particle-sizing instruments, are not designed to assess particle shapes. Special methods requiring multiple detectors are needed for this purpose, as the angular dependence of the scattered light needs to be analyzed (Kaye, 1998). Measurements of changes in the polarization state of the scattered light provide a possible alternative for nonspherical particles with a given orientation.

Here a method is presented based on the analysis of the particle dynamics in a simple shear flow of dilute systems. The particle dynamics are governed by their geometry, which determines their manner of rotation in the flow. For a given particle, the angular velocity is not constant in time. The particle slows down as its orientation approaches the flow direction. As a result of variations in angular velocities of different particles, preferred orientations develop (Okagawa et al., 1973). Frattini and Fuller (1984, 1986, 1987) and Johnson and Fuller (1988) have shown that polarimetry measurements of birefringence and especially linear conservative dichroism can be used to study the dynamics of dilute colloidal suspensions in simple shear flow. In the present work it is attempted to invert the problem and use the rheooptical response and the particle dynamics to extract information about particle geometry.

Linear conservative or scattering dichroism is a property related to anisotropic scattering of light. It is defined as the difference in the principal eigenvalues of the imaginary part of the refractive-index tensor. For the case studied here it corresponds to the volume average over the difference in scattering cross sections in two orthogonal directions (van de Hulst, 1981). In a dilute system of nonspherical particles, the

Correspondence concerning this article should be addressed to G. G. Fuller.
Current address of J. Vermant and H. Yang: Dept. of Chemical Engineering, University of California, Santa Barbara, CA 93106.

magnitude of the linear conservative dichroism reflects the degree of alignment induced by the shear flow.

In order to deduce quantitative information about the aspect ratio and the size distributions from measurements of the time-evolution of the linear conservative dichroism, assumptions about the scattering mechanism must be made in order to calculate the scattering cross sections. The selection of a scattering theory will depend on the refractive-index difference between the suspending medium and the particle, on the particle size and the shape of the particles, characteristics that are not known in advance. Even for the given type of scattering theory, the magnitude of the conservative dichroism depends in a complex manner on the size, especially when the particle size is comparable to the wavelength of the light (Meeten, 1981; Yang et al., 1998). Hence a precise calculation of size and polydispersity becomes difficult. Many of these problems can be overcome by considering the evolution of the average orientation angle χ. The latter is given by the projection of the principle axis of the imaginary part of the refractive-index tensor in the flow-velocity gradient plane. It is a purely geometrical property, the determination of which is not affected by the size for samples with uniform optical properties. For that reason it is more suited to characterizing suspensions of nonspherical particles. This is the basis of the approach followed in this article. It will be shown that an analytical expression for the time evolution of the orientation angle can be derived. The resulting equation contains only the equivalent hydrodynamic aspect ratio and the associated polydispersity as unknowns. They can be obtained from a fit to the experimental data, as will be demonstrated for a model system containing ellipsoidal hematite particles.

Theoretical Background

Single particles

In a classic paper, Jeffery (1922) solved the equations of motion for a rigid, non-Brownian ellipsoidal particle in a viscous flow at low Reynolds number. It was shown that the forces acting upon a particle reduce to two torques: one that makes the particle rotate with the vorticity of the fluid, and one that makes the particle rotate around the principal stress axes of the surrounding fluid. In a simple shear flow ($v_x = \dot{\gamma} t$, $v_y = 0$, $v_z = 0$) the principal axis of a single, neutrally buoyant, spheroid with aspect ratio r describes a motion in an Eulerian frame given by (Jeffery, 1922)

$$\tan\theta = \frac{C \cdot r}{\left(r^2 \cos^2\phi + \sin^2\phi\right)^{0.5}} \tag{1}$$

$$\tan\phi = r \cdot \tan\left(\frac{2\pi t}{T} + \kappa\right), \tag{2}$$

where θ is the first and ϕ the second Euler angle; C and κ are two integration constants that depend on the initial conditions of θ and ϕ; the constants C and κ determine the specific orbit a particle will follow; and the period of rotation $T(\phi = 0 \rightarrow 2\pi)$ is determined by the particle shape and the shear rate $\dot{\gamma}$

$$T = \frac{2\pi}{\dot{\gamma}}\left(r + r^{-1}\right). \tag{3}$$

It can be noted that the period of rotation of the particles will increase as the aspect ratio of the particles increases. Breherton (1962) showed that the rotation of a rigid axisymmetric body is mathematically identical to the result obtained by Jeffery, only r no longer represents the geometric aspect ratio of the particle, but an equivalent hydrodynamic aspect ratio defined by Eq. 3 in terms of the period of rotation. Note that r can be larger (prolate particles) or smaller (oblate particles) than one.

Equations 1 and 2 indicate that an axisymmetric body will rotate in a periodic manner, the trace of the particle being an ellipse (a Jeffery orbit). The details of the orbit will depend on the value of the so-called orbit constants C and κ. There are different particle trajectories or Jeffery orbits possible. For a dispersion containing many particles, an orientation distribution function is used.

Orientational distribution function

Okagawa et al. (1973) derived the evolution equation for the nonequilibrium, two-dimensional orientational distribution function for a suspension of monodisperse, neutrally buoyant, noninteracting rigid ellipsoids in a Newtonian medium. For an initially randomly oriented state, the time-dependent orientation distribution function (p_t) is given by

$$p_t(\theta, \phi, r) = \frac{\sin\theta}{4\pi\left[\cos^2\theta + \Lambda^2 \sin^2\theta\right]^{3/2}}, \tag{4}$$

where Λ is a function defined by

$$\Lambda^2 = \Lambda_1 \sin^2\phi + \frac{1}{2}\Lambda_2 \sin 2\phi + \Lambda_3 \cos^2\phi, \tag{5}$$

with

$$\Lambda_1 = \frac{1}{2}\left[1 + r^{-2} + (1 - r^{-2})\cos\frac{4\pi t}{T}\right] \tag{6}$$

$$\Lambda_2 = (r^{-1} - r) \cdot \sin\frac{4\pi t}{T} \tag{7}$$

$$\Lambda_3 = \frac{1}{2}\left[1 + r^2 + (1 - r^2)\cos\frac{4\pi t}{T}\right]. \tag{8}$$

Through convenient projections and averages of the orientational distribution function, a number of mechanical and optical characteristics of the suspension, such as, viscosity, normal stresses, or linear conservative dichroism, can be calculated (Okagawa et al., 1973; Frattini and Fuller, 1984). For monodisperse particles this results in material properties that will oscillate indefinitely in time during shear flow. In real systems the oscillations of the mechanical and optical properties display damped rather than undamped oscillations. Variations in particle shape and size, which lead to a polydispersity of the equivalent hydrodynamic aspect ratio, can cause these variations, as was demonstrated by Okagawa et al. (1973). When a sample is polydisperse, so-called *phase mixing* will occur, given the fact that bodies with a larger aspect ratio rotate more slowly. Gradually the correlation between the motions of the particles will be lost, as the angular velocities

of small and large particles differ. In the present work it will be assumed that the polydispersity is small and that it can be represented by a Gaussian distribution function and a standard deviation is assumed, with σ small compared to the average aspect ratio $\bar{r}$

$$g(r) = \frac{1}{(2\pi)^{0.5}\sigma} \exp\left[\frac{-(r-\bar{r})^2}{2\sigma^2}\right]. \tag{9}$$

The resulting orientational distribution function is then given by

$$p_{t,\sigma}(\theta, \phi, \bar{r}) = \int_0^\infty p_t(\theta, \phi, r)\, g(r)\, dr. \tag{10}$$

If the properties of the dispersion upon inception of flow are calculated using $p_{t,\sigma}$ the oscillations will be damped in a well-defined manner. Other causes of damping in the bulk properties include Brownian motion and particle–particle interactions. The former effect can be minimized by making measurements in the limit of high Péclet numbers. Particle–particle interactions are reduced by working with sufficiently dilute suspensions.

Rheooptical properties

The time evolution of both the linear conservative dichroism and the average particle orientation of suspensions containing model spheroids has been calculated previously in the Rayleigh (Frattini and Fuller, 1984), Rayleigh–Gans (Frattini and Fuller, 1987), and anomalous diffraction approximations (Frattini, 1985). As mentioned in the Introduction, the conservative dichroism is, however, ill-suited for treating the inverse problem, that is, to determine geometrical aspects of particles of unknown geometry and size. First, there is the need to select a scattering theory and make *a priori* assumptions about the particle geometry. Second, when a system is polydisperse, both variations in size a and shape will contribute to variations in the dichroism. *A priori* the probability distribution $p(a, r)$ cannot be simplified, assuming that variations in size and shape are independent and $p(a, r) = p_1(a) \cdot p_2(r)$. Often, but not always, changes in the size entail a change in aspect ratio and $p(a, r) = p_1(a) \cdot p_3(r|a)$. In addition to the need for the selection of a scattering theory and assumptions about the particle geometry, scattering dichroism as a characterization tool requires independent information about the probability distribution, rendering it less appropriate for this purpose.

Fortunately, the predictions for the evolution of the orientation angle have been shown to be insensitive to the choice of the light-scattering treatment. Frattini and Fuller (1987) demonstrated explicitly that the calculations in the Rayleigh and Rayleigh–Gans–Debye (RGD) produce essentially the same results. It has been verified that this also holds for the anomalous diffraction approximation (Frattini, 1985). This is not surprising, as the orientation angle is a geometric property. The independence of weighting factors involving, for example, the size, will be demonstrated by briefly recalling the calculation for the orientation angle in comparison with conservative dichroism.

A particle will interfere with the incident light wave and modify its propagation. Following van de Hulst (1981), the electric vector of the scattered light at a distance z from the particle, E_z can be related by the forward-scattering matrix $S(0)$ to the the electric vector of the incident beam E_0, by

$$E_z = \frac{e^{ikz}}{ikz} S(0) \cdot E_0, \tag{11}$$

where k is the wave number, and for the components of the forward-scattering matrix we follow the classic notation by van de Hulst (1981)

$$S(0) = \begin{vmatrix} S_2(0) & S_3(0) \\ S_3(0) & S_1(0) \end{vmatrix} \tag{12}$$

The optical properties of the suspension can be modeled by a complex refractive index tensor n. The imaginary part of this refractive index tensor is related to the forward-scattering matrix per particle by van de Hulst 1981

$$\mathrm{Im}(n) = \frac{2\pi}{k^3} n_s N\, \mathrm{Re}[S(0)], \tag{13}$$

where n_s is the refractive index of the medium and N is the number density of the scatterers. $\mathrm{Re}[S(0)]$ denotes the real part of the components of the forward-scattering matrix. The dichroism is defined as the difference between the eigenvalues of this imaginary part of n. In terms of the real part of the components of the scattering matrix, this gives

$$\Delta n'' = \frac{2\pi}{k^3} n_s N \Big(\{\mathrm{Re}[S_2(0)] - \mathrm{Re}[S_1(0)]\}^2 + 4\{\mathrm{Re}[S_3(0)]\}^2\Big)^{0.5}. \tag{14}$$

An orientation angle, specifying the principal axes of the imaginary part of n can be defined with respect to the laboratory frame

$$\tan 2\chi = \frac{2\mathrm{Re}S_3(0)}{\mathrm{Re}[S_2(0) - S_1(0)]}. \tag{15}$$

For our purpose, it is important to note that, whereas the dichroism contains a sum of the components of the scattering matrix, the orientation angle is defined as a ratio of the latter. Since the most important effects of particle size are typically contained in the prefactors to the components of $S(0)$, the dichroism will depend on particle size whereas the orientation angle will be largely insensitive to this property.

For the case of Rayleigh scatterers, the forward-scattering matrix was derived by Stoimenova et al. (1980). Substituting the components of the scattering matrix in Eq. 15 and averaging over the distribution, the time-dependent orientation angle can be calculated from (Frattini and Fuller, 1984)

$$\tan 2\chi = \frac{\langle \sin^2\theta \sin 2\phi \rangle}{\langle \sin^2\theta \cos 2\phi \rangle}, \tag{16}$$

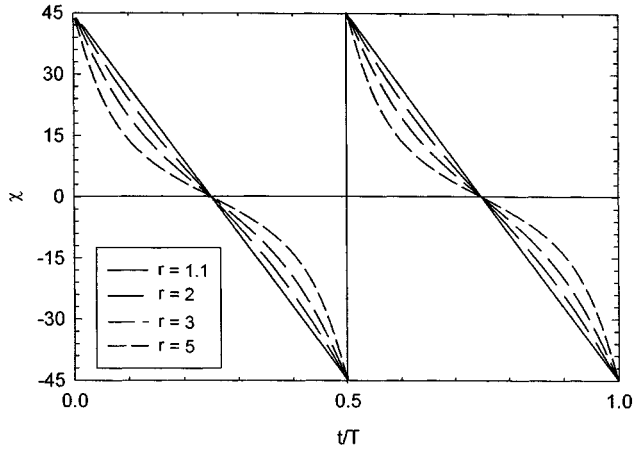

Figure 1. Evolution of average orientation angle (χ) as a function of dimensionless time (t/T) for a suspension of monodisperse prolate spheroids with different aspect ratios.

where $\langle \ldots \rangle$ denotes an average according to

$$\langle \ldots \rangle = \int_0^{\pi} \int_0^{2\pi} \ldots p_{t,\sigma}(\theta, \phi, \bar{r})\, d\phi\, d\theta. \qquad (17)$$

This integration can be carried out numerically, but is rather cumbersome, as most of the integrals are oscillatory. Figure 1 shows the evolution of the orientation angle, as a function of time, normalized by the average tumbling period, T, for different aspect ratios (prolate spheroids) after a startup of a shear flow. In these calculations, the particles are assumed to be monodisperse. As can be seen in Figure 1, the intrinsic shape of the curve changes when the aspect ratio is larger. On the average, the particles spend more time close to the flow axis when the aspect ratio is larger.

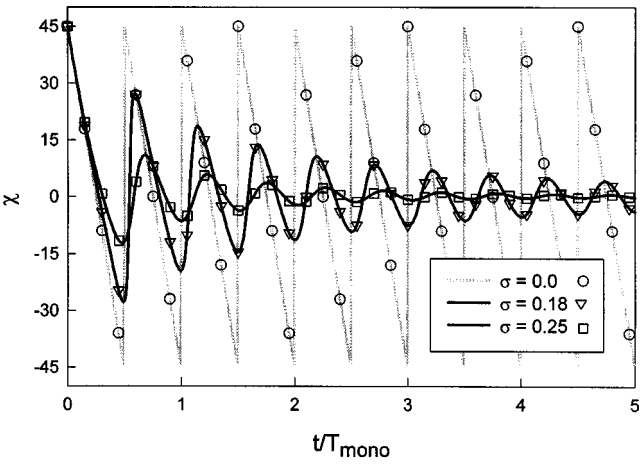

Figure 2. Evolution of average orientation angle (χ) as a function of dimensionless time (t/T) for a suspension containing spheroids of aspect ratio 0.9 and different degrees of polydispersity (σ).

With a distribution of hydrodynamic aspect ratios, the oscillations will be damped. The full numerical calculation is rather time-consuming, and is not very practical for dealing with the inverse problem. Therefore two approximations were used in order to obtain an analytical expression relating the time evolution to aspect ratio and polydispersity.

Approximation for Near Spherical Particles. When the particles are nearly spherical, $|r-1|$ is small, and from Eqs. 5–8 it follows that Λ^2 approaches unity. The probability distribution given by Eq. 4 can then be simplified using a series expansion with respect to (Λ^2-1), to yield:

$$p_t(\theta, \phi, r) = \frac{\sin\theta}{4\pi}\left[1 - \frac{3}{2}(\Lambda^2-1)\sin^2\theta\right] + \mathcal{O}\left[(\Lambda^2-1)^2\right]. \qquad (18)$$

Because (Λ^2-1) is assumed to be small, the higher-order terms can be neglected. Using this simplified form for the probability distribution function (Eq. 18), the integrations over θ and ϕ in the calculation of the orientation angle (Eq. 16) can be carried out analytically. After some algebraic manipulations, one obtains an integral equation in r:

$$\tan 2\chi = \frac{2\int_0^{\infty}(r - r^{-1})\sin\frac{4\pi t}{T}\, g(r)\, dr}{\int_0^{\infty}\left[r^2 - r^{-2} - (r^2 - r^{-2})\cos\frac{4\pi t}{T}\right] g(r)\, dr}. \qquad (19)$$

This integration still needs to be carried out numerically, but requires only about 5% of the time required to solve Eq. 16. Typical results are given in Figure 2, comparing the approximation with the full result for a prolate spheroid with an aspect ratio of 0.9 and different degrees of polydispersity. The time axis is rescaled with respect to the period of oscillation of a monodisperse system with the same average aspect ratio, T_{mono}.

Figure 2 shows how the oscillations become more strongly damped as the polydispersity increases from 0 to 0.25. Polydispersity also has a small effect on the average period of the oscillations. As the degree of polydispersity σ is increased, T slightly increases as well. This effect is most pronounced, as the aspect ratio is close to 1. In Figure 3 the ratio between the average period (T_{av}) and T_{mono} is plotted as a function of the degree of polydispersity, expressed as a standard deviation (Eq. 9) for various aspect ratios. In the worst case calculated here, that is, $r = 1.1$ and $\sigma = 0.6$, the deviation amounts to 10%. For larger aspect ratios this increase of T with σ can be neglected for all practical purposes.

Approximation for Small Polydispersities. When the assumption of nearly spherical particles is combined with an assumption that polydispersity is small, an analytical expression can be derived. Using

$$y = \frac{r - \bar{r}}{\sigma}, \qquad (20)$$

Eq. 9 can be written as:

$$g(r) = \frac{1}{2\pi\sigma}\exp\left(-\frac{y^2}{2}\right). \qquad (21)$$

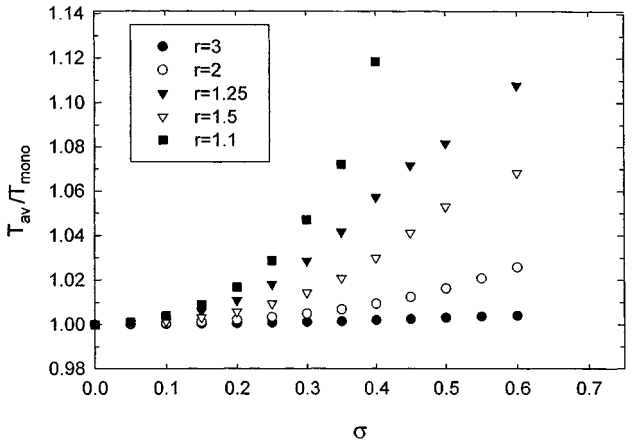

Figure 3. Ratio between average tumbling period for a polydisperse suspension (T_{av}) and oscillation period for a monodisperse system (T_{mono}) of ellipsoidal particles as a function of degree of polydispersity for various aspect ratios.

It is now assumed that σ is small compared to $\bar{r}$. The nonlinear terms in r appearing in Eq. 19 can be substituted by their approximations using terms up to the second order in y:

$$r^{-1} - r = A - By + Cy^2 + \mathcal{O}(y^3) \tag{22}$$

$$r^2 - r^{-2} = D - Ey + Fy^2 + \mathcal{O}(y^3) \tag{23}$$

$$\frac{4\pi t}{T} = \bar{\nu} t - a_2 y + a_3 y^3 + \mathcal{O}(y^3), \tag{24}$$

where

$$\bar{\nu} = \frac{2\dot{\gamma}}{\bar{r} + \bar{r}^{-1}}. \tag{25}$$

The coefficients, a_2, a_3, A, B, C, D, E, and F, are given in the Appendix. Using these approximations, the integrations in Eq. 19 can be carried out analytically. The resulting equation for the orientation angle is given by :

$$\tan 2\chi = \frac{2K}{L}. \tag{26}$$

The numerator K in Eq. 26 reduces to

$$K = \frac{1}{\sigma\sqrt[4]{1+4a_3^2}} \exp\left(-\frac{a_2^2}{2+8a_3^2}\right) \times \Bigg[A\left[\sin\bar{\nu}t\cos(\alpha) + \cos\bar{\nu}t\sin(-\alpha)\right] - B\frac{a_2}{\sqrt{1+4a_3^2}}\left[\sin\bar{\nu}t\sin(-\beta) - \cos\bar{\nu}t\cos(-\beta)\right] + C\frac{1}{\sqrt{1+4a_3^2}}\left\{\sin\bar{\nu}t\left[\cos(\beta) - \frac{a_2^2}{\sqrt{1+4a_3^2}}\cos(\gamma)\right] + \cos\bar{\nu}t\left[\sin(-\beta) - \frac{a_2^2}{\sqrt{1+4a_3^2}}\sin(-\gamma)\right]\right\}\Bigg]. \tag{27}$$

The coefficients α, β, and γ are given in the Appendix. The denominator L in Eq. 26 reduces to

$$L = \frac{1}{\sigma}\left[\bar{r}^2 - \bar{r}^{-2} + (1-3\bar{r}^{-4})\sigma^2\right] - \frac{1}{\sqrt{2\pi}\sigma}M, \tag{28}$$

with M

$$M = \frac{\sqrt{2\pi}}{\sqrt[4]{1+4a_3^2}} \exp\left(-\frac{a_2^2}{2+8a_3^2}\right) \times \Bigg[D\left[\cos\bar{\nu}t\cos(\alpha) - \sin\bar{\nu}t\sin(-\alpha)\right] + E\frac{a_2}{\sqrt{1+4a_3^2}}\left[\cos\bar{\nu}t\sin(-\beta) + \sin\bar{\nu}t\cos(\beta)\right] + F\frac{1}{\sqrt{1+4a_3^2}}\left\{\cos\bar{\nu}t\left[\cos(\beta) - \frac{a_2^2}{\sqrt{1-4a_3^2}}\cos(\gamma)\right] + \sin\bar{\nu}t\left[\sin(-\beta) - \frac{a_2^2}{\sqrt{1+4a_3^2}}\sin(-\gamma)\right]\right\}\Bigg]. \tag{29}$$

Once $\bar{r}$ is estimated from T, the polydispersity σ is the only unknown in Eq. 26 and can be used as a fitting parameter to describe the experimentally observed curves.

To evaluate the different calculation procedures, the results of the full numerical calculation of Eq. 16 are compared in Figure 4 with the different approximations for a suspension containing particles with an aspect ratio of 2 and a shape polydispersity of 0.2. The approximation for near-spherical particles, given by Eq. 19, still has to be solved numerically. The results are nearly identical to the exact result with a reduction of the computational effort. The analytical expression obtained by furthermore assuming small polydispersity and approximating the non-linear terms up to the second order (Eq. 26) gives very good results. It will be referred to as the second-order approximation.

To test the limits of the applicability of the second-order approximation in a more detailed manner, the results of the full numerical calculation were compared with the results obtained by using Eq. 26 for various sets of values ($\bar{r}$, σ). Figure 5a gives the evolution of the orientation angle upon startup of a shear flow for an initially random oriented system with an average aspect ratio of 5 and a varying degree of polydispersity. The symbols in Figure 5 give the results of the full numerical calculation of Eq. 16. The lines represent the ana-

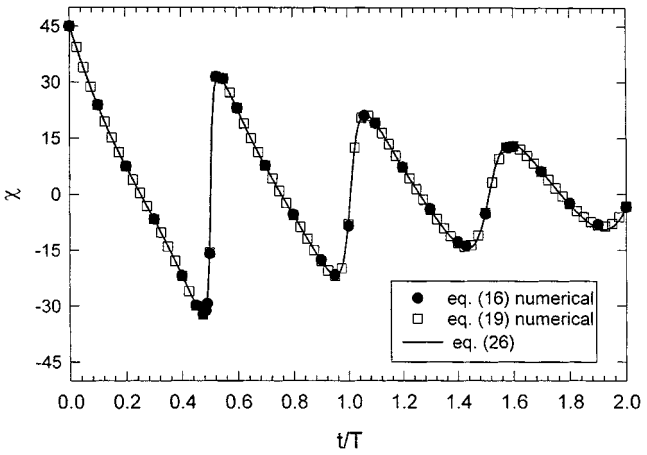

Figure 4. Calculations of the evolution of orientation angle (χ) as a function of dimensionless time (t/T) using the full numerical solution of Eq. 16, numerical solution of Eq. 19, and analytical solution using second-order approximations of Eq. 26.

lytical expression of Eq. 26. Even beyond the strict limits of validity of the second-order approach, the curves generated by this approximation describe the evolution of the orientation angle very well. At the highest degree of polydispersity calculated here, $\sigma = 0.6$, the agreement between Eq. 26 and the full numerical result becomes slightly less accurate, especially at longer times ($t/T > 1.5$). The analytical result then predicts an evolution that is less damped than the full numerical result. However, the first period of the damped oscillation is well described. Figure 5b compares the analytical approximation (lines) with the full numerical results (symbols) at a given degree of polydispersity of 0.2. Even up to aspect ratios of 10, the second-order approximation gives good results.

Particle characterization method

The method proposed in this work is therefore to use the rheooptical response of a dilute system, and the analytical equations presented earlier to determine the equivalent hydrodynamic aspect ratio and polydispersity of nonspherical particles as they are dispersed in the fluid. The shear rates at which the dispersions are sheared must be such that the hydrodynamic forces dominate the thermal forces associated with Brownian motion, that is, in the high Péclet regime. The sample should be sufficiently dilute to avoid two-body interactions, but still provide sufficient scattering contrast. The *equivalent hydrodynamic aspect ratio* of the particles and the associated polydispersity can be obtained by using Eq. 26 to fit the evolution of the orientation angle upon inception of a shear flow at high Péclet numbers.

Conservative dichroism can be applied in another way to productively characterize the particles. The *size* can be obtained from the measurement of the rotational diffusivity, D_r. The latter can be obtained from the relaxation of the dichroism or orientation angle after cessation of flow (Frattini and Fuller, 1986). The orientation will be gradually lost, due to Brownian motion. The relaxation behavior will be described by a decreasing exponential, the relaxation time being $(6D_r)^{-1}$. The rotational diffusivity is related to the aspect ratio and particle size, and a detailed discussion is given by Brenner (1974). Relating the diffusivity to the particle size requires the knowledge of the medium viscosity.

The use of the method for determining the equivalent hydrodynamic aspect ratio and polydispersity will now be demonstrated by considering a dispersion of a spindle-type hematite.

Materials and Methods

Materials

A hematite suspension was synthesized according to the method of Ozaki et al. (1984). The synthesis involved the pre-

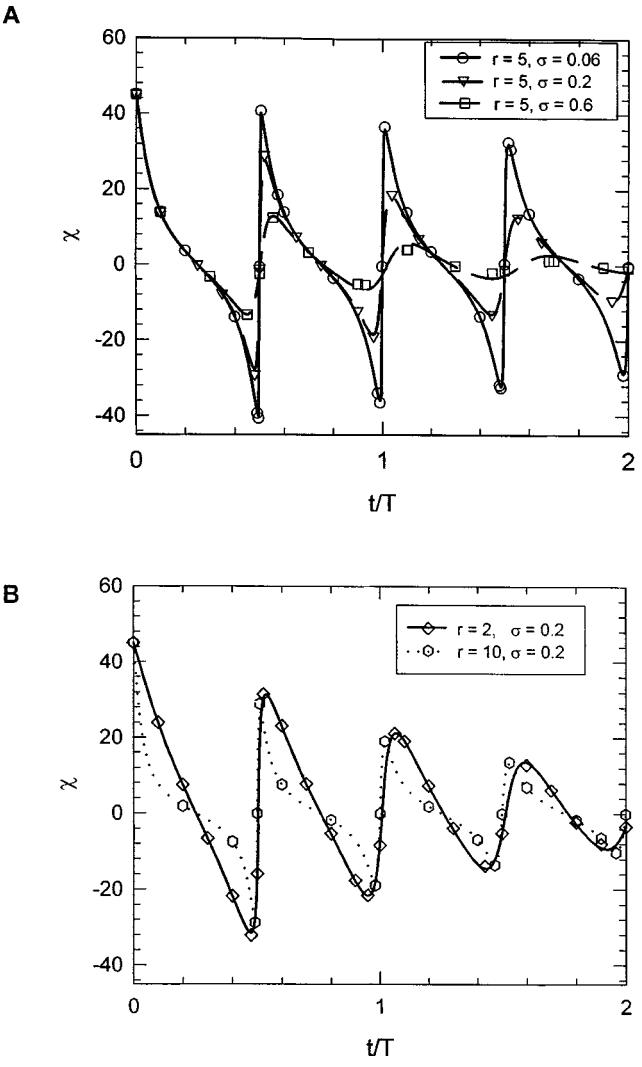

Figure 5. Evolution of average orientation angle (χ) as a function of dimensionless time (t/T).

Comparison of the full numerical calculation and the second-order approximation: (a) at a given aspect ratio of 5 and varying degree of polydispersity (σ) of 0.05, 0.2, and 0.6; (b) at a given degree of polydispersity of 0.2 and aspect ratios (r) of 2 and 10.

cipitation of hematite from an aqueous solution of 4×10^{-4} M sodium phosphate and 0.02 M ferric floride by forced hydrolysis of the ferric salt. A volume of 5 cm^3 of 1.0 M HCl was added to 200 cm^3 of the dispersion, aiming for an aspect ratio of 2 to 3 (Ozaki et al., 1984). The samples were aged at 100°C for 72 h in an air oven. Precipitates were subsequently centrifuged and washed several times with bidistilled water and stored. Subsequently, dispersions were prepared in mixtures of glycerol and water. Glycerol is added to increase the medium viscosity in order to reduce the particle diffusivity, rendering the regime where the hydrodynamic forces dominate more accessible for our experiments. The viscosity of the glycerol–water mixture is only important when one wants to obtain the particle size from the measurement of the rotational diffusivity. It was observed that stable dispersions could be prepared in a slightly acidic medium by sonicating the dispersions with regular intervals, as demonstrated by Boger and coworkers (Solomon and Boger, 1988, Gason et al., 1999). The hematite particles can be approximated as being intrinsically optically isotropic, the difference between the principal refractive differences being smaller than 10%, as was shown by Johnson and Fuller (1988).

The physical dimensions of the particles were investigated by scanning electron microscopy (SEM). Figure 6 shows a typical scanning electron micrograph of gold-coated particles, indicating their ellipsoidal nature. A geometric aspect ratio was defined as the ratio between the lengths of the major and minor axis for each particle. Such a definition does not account deviations in particle shape from ellipsoids, which are nevertheless present. The distribution of these aspect ratios could be described by a Gaussian curve with a mean value $\bar{r}$ of 2.50 and a standard deviation σ of 0.25, averaged over 60 particles. The particles had an average major axis of 430 ± 50 nm and a minor axis of about 170 ± 20 nm.

Experimental Method

A polarization modulation method was used to measure simultaneously the linear dichroism and the orientation angle as a function of time. A rheometrics optical analyzer (ROA) was used for this purpose. It is based on a rotary polarization modulation principle as suggested by Fuller and Mikkelsen (1989). The optical train consists of a polarizer and a half-wave plate rotating at a frequency ω of 2 kHz, which provides a modulation of the incoming light at a frequency of 8 kHz. For a dichroic sample, in the limit of small anisotropies, the intensity of the light transmitted by the sample is given by (Fuller, 1995):

$$I=\frac{I_0}{2}\left[\cosh\delta''-(\cos2\chi\sinh\delta'')\cos4\omega t-(\sin2\chi\sinh\delta'')\sin4\omega t\right], \quad (30)$$

with I_0 the intensity of the incoming light, χ the orientation angle, and δ'' the extinction. The "DC" part of the transmitted light intensity ($I_0/2\cosh\delta''$) is filtered out by using a low-pass filter. Phase-sensitive detectors (lock-in amplifiers, Stanford Research Systems Model 530) are used to determine the in-phase and out-of-phase components of the light intensity transmitted by the sample. From the measured values of I_{DC}, $I_{\cos4\omega t}$, and $I_{\sin4\omega t}$, the orientation angle χ and the magnitude of the dichroism $\Delta n''$ can be determined simultaneously. The high modulation frequency makes it possible to study fast time-dependent phenomena. Other optical trains using photoelastic modulators are possible. More details on this technique are given by Fuller (1995). A Couette cell is used here to probe the anisotropy in the flow-velocity gradient plane as light is sent down the vorticity direction. The path length of the beam through the Couette flow cell is 2.44 cm.

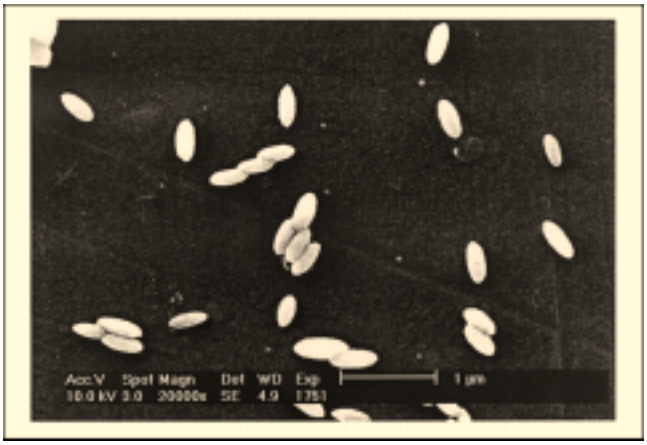

Figure 6. SEM micrograph of hematite particles.

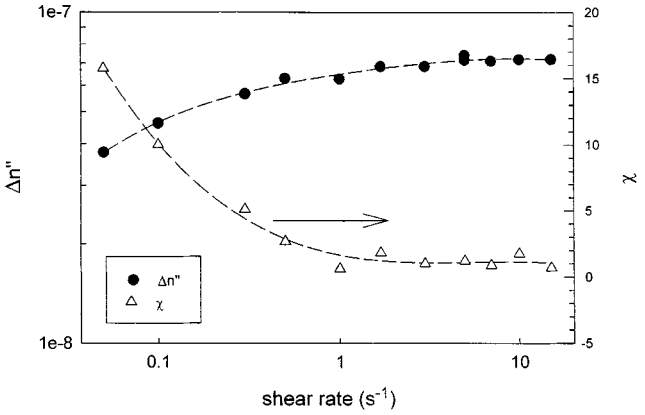

Figure 7. Conservative dichroism ($\Delta n''$) and orientation angle (χ) as a function of shear rate for a 35-ppm suspension of hematite in a 5% water/95% glycerin mixture.

Results

Steady state

Figure 7 shows the conservative dichroism and orientation angle observed under steady-state flow conditions for a dilute suspension of about 35 ppm of the hematite sample in a 5/95 water–glycerin mixture. At low shear rates, the effect of Brownian motion is to render the orientation distribution more isotropic. The magnitude of the dichroism is small and the orientation angle differs from zero. As the shear rate is

increased, the shear flow is capable of orienting the particles, the magnitude of the dichroism increases, and the orientation angle decreases gradually down to 0°. This indicates the regime where the hydrodynamic forces dominate. In the following, we will only present results that were taken in this regime. At very high shear rates, at particle Reynolds numbers approaching 1, the particle inertia will become important. From an experimental point of view this can be assessed from the transient behavior (see below). The steady-state data are hence useful in determining the lower shear-rate limit at which the high Péclet regime is reached. For the present sample the lower shear-rate limit was found to be 1 s^{-1}.

Transient data

In the transient experiments, flow is started up from an initially randomly oriented sample. This initial state can be produced in the current samples by allowing the sample to relax over a sufficient time scale, being rendered isotropic by Brownian motion. The random orientation state can be detected from the rheooptical response, as all optical anisotropy should vanish. The damped oscillatory response for the conservative dichroism in the high Péclet regime together with the evolution of the orientation angle are shown in Figure 8 for startup experiments at five different shear rates between 1 and 7 s^{-1}. The dichroism was re-scaled with respect to its steady-state value ($\Delta n''_{SS}$). The data for both dichroism and orientation angle obtained at different shear rates superimpose when plotted as a function of the strain. At higher shear rates (not shown here), this scaling fails, indicating the point at which particle inertia becomes important or instrumental artifacts due to the motor and drive belt occur. For the present sample this occurred at about 15 s^{-1}. A damped oscillatory behavior is observed in the shear-rate range between 1 and 10 s^{-1}, and up to three oscillations are clearly visible.

The evolution of the orientation angle could be described fairly well by Eq. 26, and the resulting fit is shown in Figure 8b by the full line. The best-fit parameters yielded an equivalent hydrodynamic aspect ratio of 1.75 and an associated polydispersity of 0.65. The value of 1.75 for the equivalent aspect ratio is lower than the value of 2.5 obtained for the geometric aspect ratio from the SEM images, and the associated polydispersity of 0.65 is larger than the value of 0.25 obtained from the SEM analysis. This discrepancy is not surprising, as the aspect ratio and polydispersity given by the rheooptical method are the equivalent hydrodynamic ones. Deviations from an ellipsoidal shape will lower the equivalent hydrodynamic aspect ratio and increase the associated polydispersity. As can be observed in Figure 6, some of the particles are not perfectly ellipsoidal. Additionally, the presence of small aggregates consisting of two or three particles in the dispersion cannot be excluded. These aggregates will have a smaller effective aspect ratio. The particles used in the present work were not sterically stabilized, and a complete dispersion is not assured, especially not in glycerin/water mixtures stabilized by electrostatics only. Both variations in shape and the presence of small aggegrates will result in a lower effective hydrodynamic aspect ratio and lead to an increased polydispersity as compared to the data obtained from the SEM analysis.

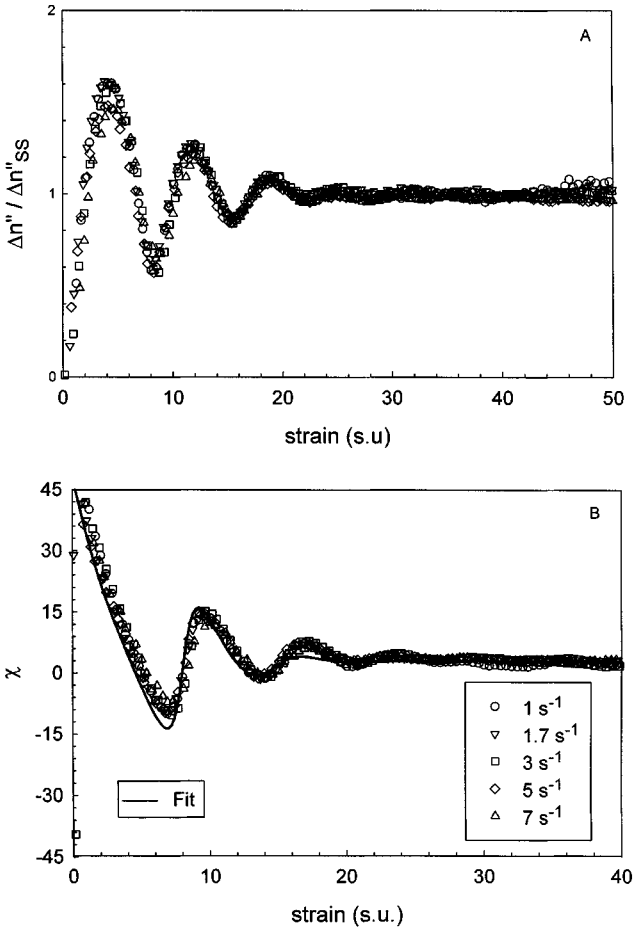

Figure 8. (a) Conservative dichroism ($\Delta n''$) and (b) orientation angle (χ) as a function of strain for 35 ppm suspensions of hematite in 5/95 water/glycerin mixtures at five different shear rates.

Only one out of four data points is shown; the full line is a fit of Eq. 26.

It should be pointed out that the rheooptical method produces the more relevant characteristics, the experimental aspect ratio and polydispersity referring to the hydrodynamic rather than the purely geometric properties of the particles. For many practical applications, it is only these equivalent hydrodynamic factors that govern the suspension behavior, for instance rheology or sedimentation. Relating geometric to hydrodynamic properties is not straightforward for real particles, which cannot be described by perfect mathematical bodies.

Conclusions

A method has been presented to determine the equivalent hydrodynamic aspect ratio and associated polydispersity for axisymmetric nonspherical particles dispersed in a medium. The time evolution of the average orientation angle of dilute suspensions of nonspherical particles upon inception of a shear flow is monitored by means of the polarization modulation method. Because the orientation angle is a geometric property, the time evolution of the orientation angle is essen-

tially dependent on two parameters: the equivalent hydrodynamic aspect ratio, and associated polydispersity. An analytical expression has been derived under the assumption that the particles are axisymmetric, have isotropic optical properties, are sufficiently dilute, have aspect ratios that are below 10 and relatively small polydispersity, and that the suspension is sufficiently dilute. The advantages of the present method are that it is rapid, and that the experimentally determined aspect ratio refers to the hydrodynamic properties of the particles pertaining to the dispersion as such; these are the relevant properties for a number of applications. The usefulness of the technique has been demonstrated by determining the aspect ratio and polydispersity in a model hematite sample.

Acknowledgments

The financial support of Elf Aquitaine during part of this work is gratefully acknowledged. One of the authors (J.V.) is a Post-Doctoral research fellow of the Fund for Scientific Research - Flanders (FWO-Vlaanderen).

Prof. Matijević is acknowledged for suggesting the preparation procedure of the hematite sample. Prof. Norman Wagner and Prof. Jan Mewis are thanked for stimulating discussions.

Literature Cited

Breherton, F. P., "The Motion of Rigid Particles in a Shear Flow at Low Reynolds Number," *J. Fluid. Mech.*, **14**, 284 (1962).

Brenner, H., "Rheology of a Dilute Suspensions of Axisymmetric Particles," *Int. J. Multiphase Flow*, **1**, 195 (1974).

Frattini, P. L., and G. G. Fuller, "The Dynamics of Dilute Colloidal Suspensions Subject to Time Dependent Flow Fields by Conservative Dichroism," *J. Colloid Interface Sci.*, **100**, 506 (1984).

Frattini, P. L., PhD Thesis, Stanford Univ., Stanford, CA (1985).

Frattini, P. L. and G. G. Fuller, "Rheo-Optical Studies of the Effect of Weak Brownian Rotations in Sheared Suspensions," *J. Fluid Mech.*, **168**, 119 (1986).

Frattini, P. L., and G. G. Fuller, "Conservative Dichroism of a Sheared Suspension in the Rayleigh-Gans Light Scattering Approximation," *J. Colloid Interface Sci.*, **119**, 335 (1987).

Fuller, G. G., and K. J. Mikkelsen, "Note: Optical Rheometry Using a Rotational Polarization Modulator," *J. Rheol.*, **33**, 761 (1989).

Fuller, G. G., *Optical Rheometry of Complex Fluids*, Oxford Univ. Press, Oxford (1995).

Gason, S. J., D. V. Boger, and D. E. Dunstan, "Rheo-optic Measurements on Dilute Suspensions of Hematite Rods," *Langmuir*, **15**, 7446 (1999).

Hiemenz, P. C., and R. Rajagopalan, *Principles of Colloid and Surface Chemistry*, 3rd ed., Dekker, New York (1997).

Jeffery, G. B., "The Motion of Ellipsoidal Particles Immersed in a Viscous Fluid," *Proc. Roy Soc. Ser. A*, **102**, 161 (1922).

Johnson, S. J., and G. G. Fuller, "The Optical Anisotropy of Sheared Hematite Suspensions," *J. Colloid Interface Sci.*, **124**, 441 (1988).

Kaye, P. H., "Spatial Light-Scattering Analysis as a Means of Characterizing and Classifying Non-Spherical Particles," *Meas. Sci. Technol.*, **9**, 141 (1998).

Meeten, G. H., "Conservative Dichroism in the Rayleigh-Gans-Debye Approximation," *J. Colloid. Interface Sci.*, **84**, 235 (1981).

Okagawa, A., R. G. Cox, and S. G. Mason, "The Kinetics of Flowing Dispersions, VI. Transient Orientation and Rheological Phenomena of Rods and Discs in Shear Flows," *J. Colloid Interface Sci.*, **43**, 303 (1973).

Ozaki, M., S. Kratrohvil, and E. Matijević, "Formation of Monodispersed Spindle-Type Hematite Particles," *J. Colloid Interface Sci.*, **102**, 146 (1984).

Solomon, M. J., and D. V. Boger, "The Rheology of Aqueous Dispersions of Spindle-Type Colloidal Rods," *J. Rheol.*, **42**, 929 (1998).

Stoimenova, M., L. Labiki, and S. Stoylov, "Orientationally Induced Dichroism in Dilute Disperse Systems," *J. Colloid Interface Sci.*, **77**, 53 (1980).

van de Hulst, H. C., *Light Scattering by Small Particles*, Dover, New York (1981).

Yang, H., H. Zhang, P. Moldenaers, and J. Mewis, "Rheo-Optical Investigation of Immiscible Polymer Blends", *Polymer*, **39**, 5731 (1998).

Appendix

The coefficients used to evaluate Eq. 26 are :

$$a_2 = \frac{2\,\dot{\gamma} t(1-\bar{r}^{-2})\sigma}{(\bar{r}+\bar{r}^{-1})^2} \tag{A1}$$

$$a_3 = \frac{2\dot{\gamma} t(1-3\bar{r}^{-2})\sigma^2}{(\bar{r}+\bar{r}^{-1})^3} \tag{A2}$$

$$A = \bar{r}^{-1} - \bar{r} \tag{A3}$$

$$B = (1+\bar{r}^{-2})\sigma \tag{A4}$$

$$C = \bar{r}^{-3}\sigma^2 \tag{A5}$$

$$D = \bar{r}^2 - \bar{r}^{-2} \tag{A6}$$

$$E = (2\,\bar{r} + 2\bar{r}^{-3})\sigma \tag{A7}$$

$$F = (1-3\bar{r}^{-4})\sigma^2 \tag{A8}$$

$$\alpha = \frac{a_2^2 a_3}{1+4a_3^2} - \frac{\arctan(2\,a_3)}{2} \tag{A9}$$

$$\beta = \frac{a_2^2 a_3}{1+4a_3^2} - \frac{3\arctan(2\,a_3)}{2} \tag{A10}$$

$$\gamma = \frac{a_2^2 a_3}{1+4a_3^2} - \frac{5\arctan(2\,a_3)}{2} \tag{A11}$$

Manuscript received Jan. 11, 2000, and revision received Sept. 7, 2000.